15th Triennial World Congress, Barcelona, Spain

ADAPTIVE REJECTION OF ECCENTRICITY TENSION DISTURBANCES IN WEB TRANSPORT SYSTEMS

Yulin Xu, Michel de Mathelin, Dominique Knittel

Strasbourg I University, ERT-Enroulement, LSIIT-UMR CNRS 7005
ENSPS, Bd. Sébastien Brant, 67400 Illkirch, FRANCE
Tel: +33 (0)3 90 24 44 70 Fax: +33 (0)3 90 24 44 80
e-mail: michel.demathelin@ensps.u-strasbg.fr
http://gravir.u-strasbg.fr http://ert-enroulement.u-strasbg.fr

Abstract: This paper presents adaptive algorithms to compensate roll eccentricity perturbations in web transport systems. Roll eccentricity creates tension disturbances whose frequencies may be slowly varying due to the change of radius of the roll. The magnitude and phase of these perturbations are estimated through an adaptive algorithm that cancels the effect of these perturbations. The ability of the algorithm to reject eccentricity perturbations with slowly varying frequencies is shown through simulations on the physical model, as well as experimental results.

Keywords: Roll eccentricity perturbations, disturbance rejection, web transport, adaptive algorithm.

1. INTRODUCTION

We study a system that is quite common in industry. The system has at least three motors (cf. Figure 1): an unwinder, a traction motor and a winder, and it presents the inherent difficulties of web transport systems. An important control problem in web transport systems is the effect of the perturbations due to the eccentricity of the rolls. In web transport systems, roll eccentricity creates tension disturbances that are periodic or quasi-periodic due to change of radius of the roll when the roll is the winder or the unwinder. These perturbations can sometimes induce web break and folds or material damage. This paper focuses on removing the effect of these disturbances that are quasi-periodic (periodic with a slowly varying frequency) and whose amplitude and phase are unknown. There exist several approaches to tackle this problem. One is based on repetitive control principles (see, e.g., (Garimella and Srinivasan, 1994), (Hillerström, 1996), (Lee and Smith, 1998), (Weiss and Häfele, 1999)). Another approach is based on adaptive algorithms (see, e.g., (Bodson and Douglas, 1997), (Bodson *et al.*, 1998), and (Canudas de Wit and Praly, 1998)). In our application (high speed web transport), it is important to design an algorithm that can be added to an existing industrial controller. Therefore, we propose two adaptive algorithms based on the adaptive algorithms for noise cancellation of (Bodson and Douglas, 1997). These algorithms lock on the amplitude and phase of the perturbations and cancels their effect.

The paper is organized as follows, the first section presents the model of the web transport system based on the laws of physics. The second section describes two adaptive algorithm schemes that reject the effect of quasi-periodic perturbations. The last section shows simulations and preliminary practical results when these algorithms are applied to web transport systems.

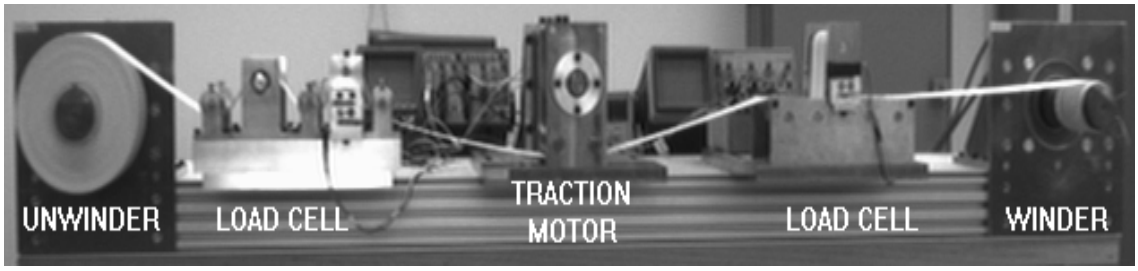

Fig. 1. Experimental setup

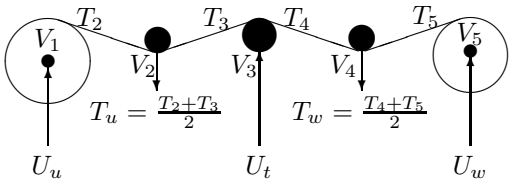

Fig. 2. Three motors web transport system

2. MODEL OF THE WEB TRANSPORT SYSTEM

Figure 2 shows a typical three motors system with winder, unwinder, tractor and two load cells that is used for our experiments. The complete model of this system is given by the following equations (see, e.g., (Koç, 2000) and (Koç *et al.*, 2000)):

Tensions between consecutive rolls:

$$L_{k-1}\frac{dT_k}{dt} = ES(V_k - V_{k-1}) + T_{k-1}V_{k-1} - T_k(2V_{k-1} - V_k) \quad (1)$$
$$k = 2,3,4,5 \quad (V_k = R_k\Omega_k)$$

where L_{k-1} is the web length between roll $k-1$ and roll k, T_k is the tension on the web between roll $k-1$ and roll k, V_k is the linear velocity of the web on roll k, Ω_k is the rotational speed of roll k, R_k is the radius of roll k, E is the Young modulus and S is the web section.

Laws of motion:

Unwinder: $(U_1 = U_u)$

$$\frac{d(J_1\Omega_1)}{dt} = R_1T_2 - K_1U_u - C_{fu} - f_{vu}\Omega_1 \quad (2)$$

Unwinder load cell:

$$J_2\frac{dV_2}{dt} = R_2^2(T_3 - T_2) - f_2V_2 \quad (3)$$

Tractor: $(U_3 = U_t)$

$$J_3\frac{d\Omega_3}{dt} = R_3(T_4 - T_3) + K_3U_t - C_{ft} - f_{vt}\Omega_3 \quad (4)$$

Winder load cell:

$$J_4\frac{dV_4}{dt} = R_4^2(T_5 - T_4) - f_4V_4 \quad (5)$$

Winder: $(U_5 = U_w)$

$$\frac{d(J_5\Omega_5)}{dt} = -R_5T_4 + K_5U_w - C_{fw} - f_{vw}\Omega_5 \quad (6)$$

where C_{fw}, C_{ft}, C_{fu} are the dry friction torques of the three motors, respectively, f_{vu}, f_{vt} and f_{vw} are the viscous friction coefficients, and K_kU_k are the motor torques. We can notice that the inertia J_k and the radius R_k of the winder and the unwinder,are time dependent and may vary on a large scale during the process operation (about 300 % for the radius in our experiments).

The effect of the eccentricity of roll k can be modeled as a sinusoidal perturbation on the nominal radius of roll k:

$$R_k(t) = R_{0k}(t) + A_k sin(\theta_k(t)) \quad (7)$$

where $R_{0k}(t)$ is the nominal radius of roll k and:

$$\theta_k(t) = \int_{t_0}^{t} \Omega_k d\tau + \delta\theta_k(t) \quad (8)$$

Where $\delta\theta_k(t)$ is a slowly varying phase-shift. In a constant speed web transport system, if the eccentricity perturbation is on the winder or the unwinder, the perturbation frequency is shifting with time due to the change of nominal radius of the roll. This model has been validated experimentally on the system shown in Figure 1. The

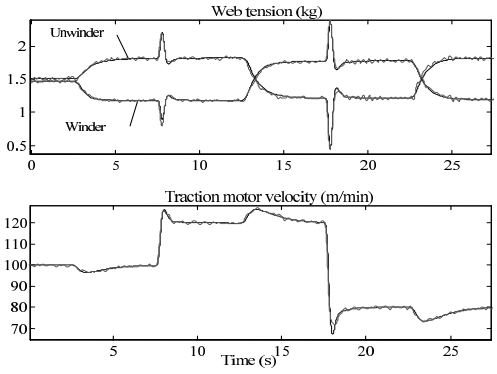

Fig. 3. Model matching

matching performed is excellent as it can be seen in Figure 3, without perturbation.

3. ADAPTIVE PERTURBATION REJECTION

We present two adaptive algorithms for the rejection of eccentricity perturbations. These algorithms are based on the work of Bodson (see, e.g., (Bodson and Douglas, 1997) and (Bodson, 1998)) on noise cancellation. The main difference between these two algorithms is the type of identifed noise parameters.

3.1 *Adaptive algorithm I*

This algorithm is based on a phase-locked loop structure that estimates simutaneously the phase and magnitude of the perturbation and then cancels it. This algorithm can be seen as a modified version of a structure used in frequency demodulation. We adapt Bodson's approach to the case of a feedback control system with output signal y and reference input signal r instead of the case of a noise cancellation system. Another difference with Bodson's approach is that the central frequency Ω_c of the perturbation can be measured and added at the input of the frequency modulator in the loop. The adaptive algorithm scheme is shown

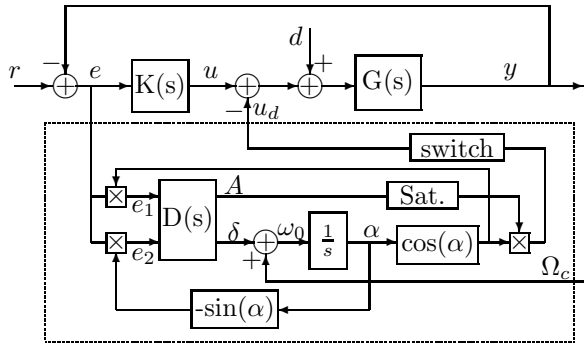

Fig. 4. Adaptive algorithm scheme I

in Figure 4, where G(s) is the system, K(s) is the controller, d is the unknown quasi-periodic perturbation (assumed to be equivalent to the eccentricity perturbation), A is the estimate of the magnitude of the perturbation, ω_0 is the estimate of the instantaneous frequency of the perturbation and α is the estimate of its phase. Therefore, if u_d is the estimate of the perturbation, then:

$$u_d = Acos(\alpha) \tag{9}$$

with

$$\dot{\alpha} = \omega_0 = \delta + \Omega_c \tag{10}$$

It's important that the perturbation cancellation algorithm does not make matter worse even during a starting transient. Therefore, we modify Bodson's algrithm by introducing a saturation block on the estimated magnitude A and a switching system that can slowly close or open the perturbation cancellation loop. The transfer function matrix D(s) relates the error signals e_1 and e_2 to the estimated magnitude A and estimated frequency shift δ, respectively. An approximate analysis of this adaptive algorithm will allow us to deduce a simple design rule for $D(s)$. This harmonic analysis is based on the following assumptions:

- The value of A, δ and Ω_c varies sufficiently slowly, so that the response of the feedback system to the signal $u_d(t)$ can be approximated by the steady-state output of the system for a sinusoidal input with the frequency ω_0. This is a standard assumption in demodulation systems.
- The instantaneous frequency $\omega_0 = \dot{\alpha}$ is close to the known frequency Ω_c so that $G(j\omega_0)$ can be replaced by $G(j\Omega_c)$.

We make the assumption that the perturbation to be cancelled is equivalent to an input pertubation, $d(t) = A_d(t)cos(\alpha_d(t))$. Therefore,

$$\begin{aligned} y &= \frac{KG}{1+KG}[r] - \frac{G}{1+KG}[u_d - d] \\ e &= \frac{1}{1+KG}[r] + \frac{G}{1+KG}[u_d - d] \end{aligned} \tag{11}$$

Let's define:

$$\begin{aligned} G_R &= Re[\frac{G}{1+KG}(j\Omega_c)] \\ G_I &= Im[\frac{G}{1+KG}(j\Omega_c)] \end{aligned}$$

If we neglect the transient due to the variations of A, δ, Ω_c, we have:

$$\begin{aligned} e = &\frac{1}{1+KG}[r] + AG_R cos(\alpha) - AG_I sin(\alpha) \\ &-A_d G_R cos(\alpha_d) + A_d G_I sin(\alpha_d) \end{aligned} \tag{12}$$

$$\begin{aligned} e_1 = &\frac{1}{2}AG_R + \frac{1}{2}AG_R cos(2\alpha) - \frac{1}{2}AG_I sin(2\alpha) \\ &+cos(\alpha)\frac{1}{1+KG}[r] - \frac{1}{2}A_d G_R cos(\alpha - \alpha_d) \\ &-\frac{1}{2}A_d G_I sin(\alpha - \alpha_d) - \frac{1}{2}A_d G_R cos(\alpha + \alpha_d) \\ &+\frac{1}{2}A_d G_I sin(\alpha + \alpha_d) \end{aligned} \tag{13}$$

$$e_2 = \frac{1}{2}AG_I - \frac{1}{2}AG_I cos(2\alpha) - \frac{1}{2}AG_R sin(2\alpha)$$

$$-sin(\alpha)\frac{1}{1+KG}[r] - \frac{1}{2}A_d G_I cos(\alpha-\alpha_d)$$
$$+\frac{1}{2}A_d G_R sin(\alpha-\alpha_d) + \frac{1}{2}A_d G_I cos(\alpha+\alpha_d)$$
$$+\frac{1}{2}A_d G_R sin(\alpha+\alpha_d) \quad (14)$$

The filter D(s) is low-pass in nature, so the high-frequency components within the system are eliminated by proper low-pass filtering of the signals e_1 and e_2. Then, the signals e_1 and e_2 are approximately given by:

$$\begin{bmatrix} e_1 \\ e_2 \end{bmatrix} = P \begin{bmatrix} A - A_d cos(\alpha-\alpha_d) \\ A_d sin(\alpha-\alpha_d) \end{bmatrix} \quad (15)$$

where P is defined as:

$$P = \frac{1}{2}\begin{bmatrix} G_R & -G_I \\ G_I & G_R \end{bmatrix} \quad (16)$$

When the phase error $\alpha-\alpha_d$ is small, this equation can be linearized as:

$$\begin{bmatrix} e_1 \\ e_2 \end{bmatrix} = P \begin{bmatrix} A - A_d \\ A_d(\alpha-\alpha_d) \end{bmatrix} \quad (17)$$

Different methods can be used to design the filter D(s). Let's define the two variables x_1 and x_2 as:

$$\begin{bmatrix} x_1 \\ x_2 \end{bmatrix} = P^{-1} \begin{bmatrix} e_1 \\ e_2 \end{bmatrix} \quad (18)$$

so that

$$x_1 = A - A_d$$
$$x_2 = A_d[\int_0^t (\delta(\sigma)+\Omega_c)d\sigma + \alpha(0) - \alpha_d(t)] \quad (19)$$

Therefore, the dynamics of the system from the

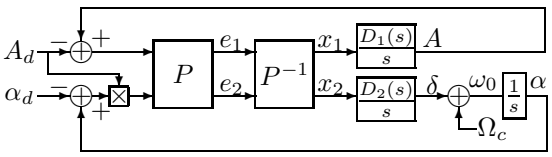

Fig. 5. Linearized model of algorithm I

parameters A and δ to the variables x_1 and x_2 are approximatively decoupled from one another and can be represented as in Figure 5. Then, D(s) may be designed as the cascade of the transformation (19) with the following filters:

$$A = \frac{D_1(s)}{s}[x_1] \quad \delta = \frac{D_2(s)}{s}[x_2] \quad (20)$$

where the integrators are included to obtain a zero steady state error on the estimate of A_d and α_d. The transfer functions $D_1(s)$ and $D_2(s)$ are designed to guarantee the closed-loop stability of the two sub-systems. According to the frequency response, $D_1(s)$ and $D_2(s)$ can be selected as:

$$D_1(s) = k_1 \leq -\frac{\bar{\Omega}_c}{10}$$
$$D_2(s) = -\frac{1}{\bar{A}_d}\frac{\bar{\Omega}_c^2}{100}\frac{(s+\bar{\Omega}_c/100)}{(s+\bar{\Omega}_c/10)} \quad (21)$$

Where $\bar{\Omega}_c$ is an average value of the system's rotation frequency Ω_c and $\bar{A}_d$ is an average value for the amplitude A_d. Because the magnitude of the disturbance A_d acts as a gain in the loop, the parameters in $D_2(s)$ must be designed for a range of magnitudes of the disturbance A_d.

3.2 *Adaptive algorithm II*

This algorithm is shown in Figure 6. It is based on the estimation of the amplitude of two components of the perturbation that are in phase quadrature to each other. The estimate of the

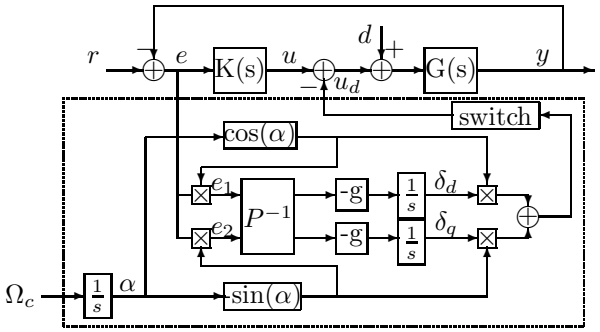

Fig. 6. Adaptive algorithm scheme II

perturbation, u_d, is given by:

$$\dot{\alpha} = \Omega_c \quad (22)$$
$$u_d = \delta_d \cos(\alpha) - \delta_q \sin(\alpha)$$

The analysis of the adaptive scheme is based on the assumption that the perturbation is equivalent to an input pertubation $d(t) = A_d(t)cos(\alpha_d(t))$. Further, we assume that the value of Ω_c varies sufficiently slowly, so that the hypothesis of algorithm I are also valid. Therefore, similarly to algorithm I, if the high-frequency terms are eliminated by proper low-pass filtering, the error signals e_1 and e_2 are approximately given by:

$$\begin{bmatrix} e_1 \\ e_2 \end{bmatrix} = P \begin{bmatrix} \delta_d - A_d \cos(\alpha-\alpha_d) \\ \delta_q + A_d \sin(\alpha-\alpha_d) \end{bmatrix} \quad (23)$$

where P is defined as in (16). Therefore, the dynamics of δ_d and δ_q are decoupled as shown in the linearized model of the disturbance cancellation loop in Figure 7. The parameter g sets the estimation dynamics. Indeed:

$$\begin{bmatrix} \dot{\delta}_d \\ \dot{\delta}_q \end{bmatrix} = -g \begin{bmatrix} \delta_d - A_d \cos(\alpha-\alpha_d) \\ \delta_q + A_d \sin(\alpha-\alpha_d) \end{bmatrix} \quad (24)$$

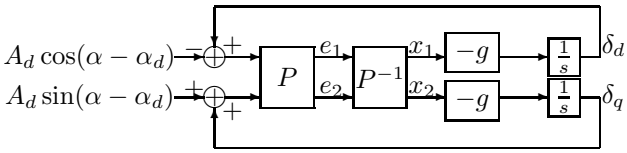

Fig. 7. Linearized model of algorithm II

Therefore, g must be $\leq \Omega_c$ in order to filter the high-pass frequency components, but large enough in order to follow the phase variations of the perturbation, d. In our experiment $g = 1 \sim 10$. In this case, δ_d exponentially converges toward $A_d\cos(\alpha-\alpha_d)$ and δ_q toward $-A_d\sin(\alpha-\alpha_d)$, so that u_d exponentially converges toward d (with time constant $\frac{1}{g}$).

4. APPLICATION TO THE WEB TRANSPORT SYSTEM

In the web transport system, if the eccentricity is due to roll k, then the main tension perturbation is on tension T_{k+1}. Therefore, we add the adaptive algorithm on the controller of the motor of roll k with a feedback of the tension T_{k+1}. For exemple, if the eccentricity is due to the unwinder, we add the adaptive perturbation cancellation algorithm on the unwinder controller as shown in Figure 8, where Ω_c is the rotation frequency of the

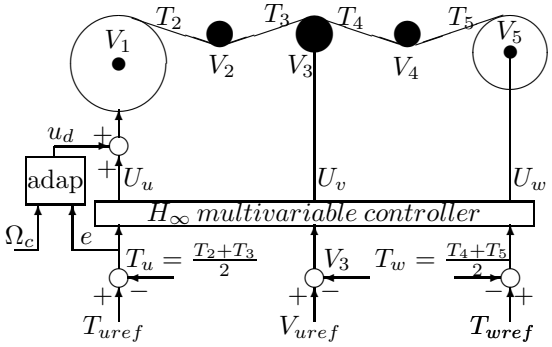

Fig. 8. Control scheme with adaptive algorithm

unwinding roll ($\Omega_c = \Omega_1$). The Bode plot of the transport function between U_u and T_u is shown in Figure 9 for different reference linear velocities V_{uref}. The controller in our experiments is designed using a H_∞ robust control approach (see (Koç *et al.*, 2000) and (Koç *et al.*, 2002)). Based on the V_{uref} value, an average value $\bar{\Omega}_c$ is computed for Ω_c and the corresponding matrix P is measured from the Bode plot. In practice, $\bar{A}_d$ is computed from the estimated amplitude A using a saturation function as in:

$$\bar{A}_d = \begin{cases} A_{min} & \text{if } A \leq A_{min} \\ A & \text{if } A_{min} \leq A \leq A_{max} \\ A_{max} & \text{if } A \geq A_{max} \end{cases} \qquad (25)$$

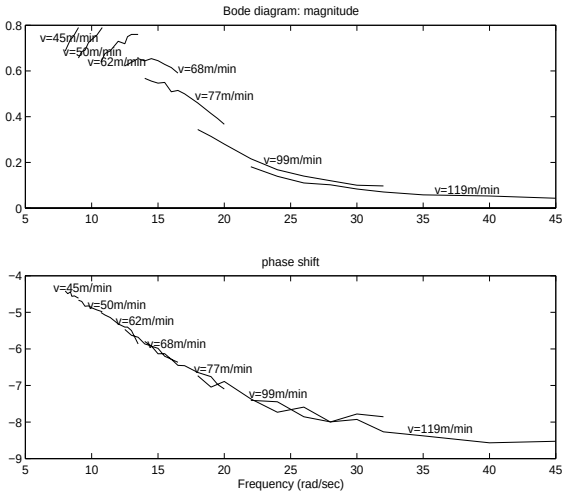

Fig. 9. Bode plot

where A_{max} and A_{min} can be selected according to the nominal output value of the controller.

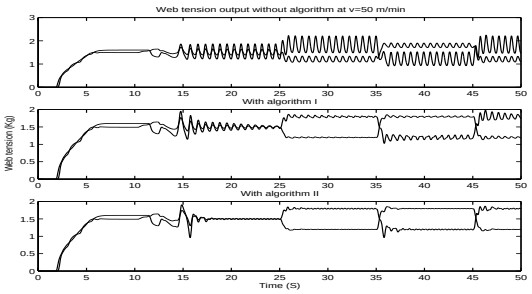

Fig. 10. Tension disturbance rejection at 50m/min

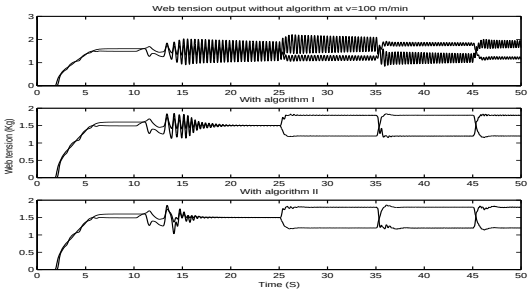

Fig. 11. Tension disturbance rejection at 100m/min

Figures 10, 11 and 12 show simulations of both algorithms rejecting an input perturbation on the unwinder roll, at the web transport speeds V_{uref} = 50 m/min, 100 m/min and 200 m/min, respectively, with a constant web tension reference signal. The cancellation algorithms is applied at time $t = 15$ sec. It can be seen that the algorithm II is more robust to tension set-point changes than the algorithm I.

Figure 13 shows the spectrogram of the web tension at the unwinder during a real experiment on

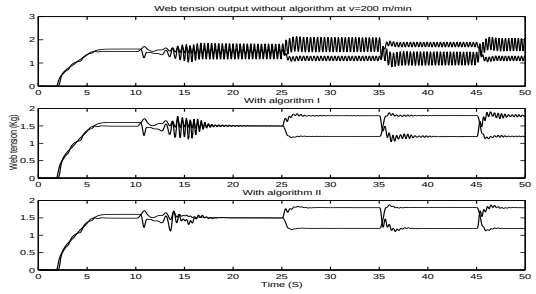

Fig. 12. Tension disturbance rejection at 200m/min

the system shown in Figure 1 for the web transport speed $V_{uref} = 50$ m/min without adaptive disturbance cancellation algorithm. Then, Figure 14 shows the spectrogram of the web tension at the unwinder during a real experiment at the web transport speed $V_{uref} = 50$ m/min with the adaptive disturbance cancellation algorithm II on the unwinder. One can see that the slowly varying

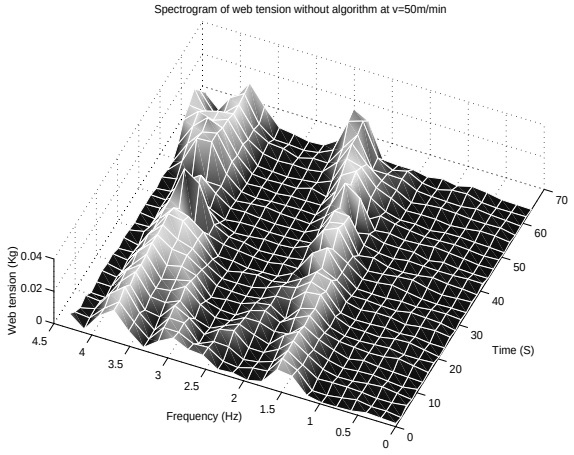

Fig. 13. Spectrogram of the web tension at 50m/min without algorithm

first harmonic is almost completely cancelled. The higher frequency perturbation term is due to the traction motor.

5. REFERENCES

Bodson, M. (1998). A discussion of Chaplin & Smith'spatent for the cancellation of repetitive vibrations. *Proceedings of the 37th IEEE Conference on Decision and Control, Tampa, Fl.*

Bodson, M. and S. C. Douglas (1997). Adaptive algorithms for the rejection of sinusoidal disturbances with unknown frequency. *Automatica.*

Bodson, M., J. S. Jensen and S. C. Douglas (1998). Active noise control for periodic disturbance. *Proceedings of the American Control Conference, Philadelphia, Pa.*

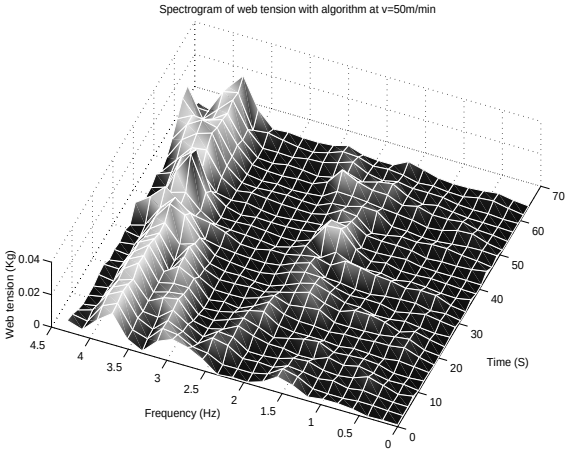

Fig. 14. Spectrogram of the web tension at 50m/min with algorithm II

Canudas de Wit , C. and L. Praly (1998). Adaptive eccentricity compensation. *Proceedings of the 37th IEEE Conference on Decision and Control, Tampa, Fl.*

Garimella, S. S. and K. Srinivasan (1994). Application of repetitive control to eccentricity compensation in rolling. *Proceedings of the American Control Conference, Baltimore, Ma.*

Hillerström, G. (1996). Adaptive suppression of vibrations–a repetitive control approach. *IEEE Transactions on control Systems Technology.*

Koç, H. (2000). Modélisation et commande robuste d'un système d'entrainement de bande flexible. PhD thesis. Université Louis Pasteur (Strasbourg I university).

Koç, H., D. Knittel, M. de Mathelin and G. Abba (2000). Robust gain-scheduling control in web winding systems. *Proceedings of the 39th IEEE Conference on Decision and Control, Sydney, Australia.*

Koç, H., D. Knittel, M. de Mathelin and G. Abba (2002). Modeling and robust control of winding systems for elastic webs. *IEEE Transactions on Control Systems Technology.* To appear.

Lee, R. C. H. and M. C. Smith (1998). Robustness and trade-offs in repetitive control. *Automatica* **34**, 889–896.

Weiss, G. and M. Häfele (1999). Repetitive control of MIMO systems using H_∞ design. *Automatica* **35**, 1185–1199.